Automating Prostate Capsule Contour Estimation for 3D Model Reconstruction Using Shape and Histological Features

Rania Hussein*, Frederic McKenzie, Ravindra Joshi

Electrical and Computer Engineering Department, Old Dominion University, VA, USA 23529

ABSTRACT

Currently there are few parameters that are used to compare the efficiency of different form of cancerous prostate surgical removal. An accurate assessment of the percentage and depth of extra-capsular soft tissue removed with the prostate by the various surgical techniques can help surgeons determining the appropriateness of surgical approaches. In order to facilitate the reconstruction phase and thus provide a more accurate quantitation results when analyzing the images, it is essential to automatically identify the capsule line that separates the prostate capsule tissue from its extra-capsular one. However the prostate capsule is sometimes unrecognizable due to the naturally occurring intrusion of muscle into the prostate gland. At these regions where the capsule disappears, its contour can be arbitrarily reconstructed by drawing a continuing contour line based on the natural shape of the prostate gland. In this paper, some mathematical equations that will be used to provide a standard prostate shape at various stages will be presented. This mathematical model can be used in deciding the missing part of the capsule. It will also be used in conjunction with Generalized Hough Transform to automatically determine the capsule line, thus provides more accurate results in the reconstruction phase as well as in the percentage of coverage and depth calculations of the extra-capsular tissue.

Keywords: Visualization, image reconstruction, 3D image quantitation, prostate surgery assessment, Generalized Hough Transform.

1. INTRODUCTION

Prostate cancer is one of the leading causes of cancer death among male population in the United States. Early detection of the disease is much more common nowadays than used to be in the past. In prostate removal surgeries, surgeons apply different removal approaches. They need to compare the quality of their different approaches as well as evaluate personal results as they relate to a standard. Thus a quantification of the prostate surgery will be very useful. Parameters that can be used to compare the efficiency of one form of surgical removal with another are the percentage and depth of extra-capsular soft tissue removed with the prostate.

The objective of this research is to facilitate and provide a more accurate and objective assessment of the percentage and depth of extra-capsular soft tissue removed with the prostate by the various surgical approaches. Assessment accuracy will be improved by developing a software algorithm to perform automatic recognition of the prostate capsule. Currently, pathologists manually perform this in order to facilitate 3D reconstruction of the prostate capsule and extra-capsular tissue. After preparing the prostate slices, pathologists hand draw the capsule boundary and place it on a separate layer to the slice information in the image manipulation software (Fig. 1). This boundary represents a contour used to reconstruct the 3D prostate model. The thickness of the hand drawn line is approximately 0.046 inches, which makes deciding whether to consider its inner or outer edge contour an issue. If the inside edge is considered, then the boundary that separates the prostate capsule from the extra-capsular tissue (which will be referred to as 'fat') might be under-estimated, while considering its outer edge might over estimate the capsule. In addition, the manual determination is a subject source of error, which can affect the accuracy of

* rhussein@odu.edu

thickness calculations of the extracapsular tissue with respect to the capsule. Error analysis and the effect of the hand-drawn boundary thickness can be found in McKenzie et al [1].

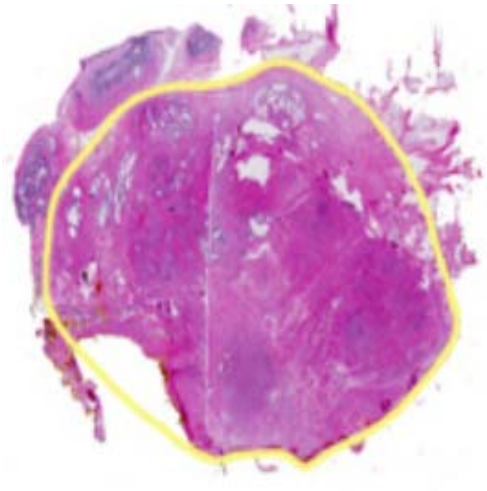

Fig. 1. A prostate slice with the hand-drawn boundary

The prostate slices used in this research are prepared using the whole mount technique. A prostate specimen is received fresh. The specimen is measured craniocaudally, antero-posteriorly and transversely and weighed. It is then dipped in water to determine its volume. The whole capsule is inked blue on the right side and red on the left to avoid any possible flipping of the slices while scanned. The capsule is then serially cut from apex to base at relatively precise and parallel 5 mm intervals in a perpendicular angle to the urethral apical orifice.

The prostate gland sits right below the bladder and is wrapped around the urethra. Figure 2 shows the basic parts of a prostate and its orientation within the human body.

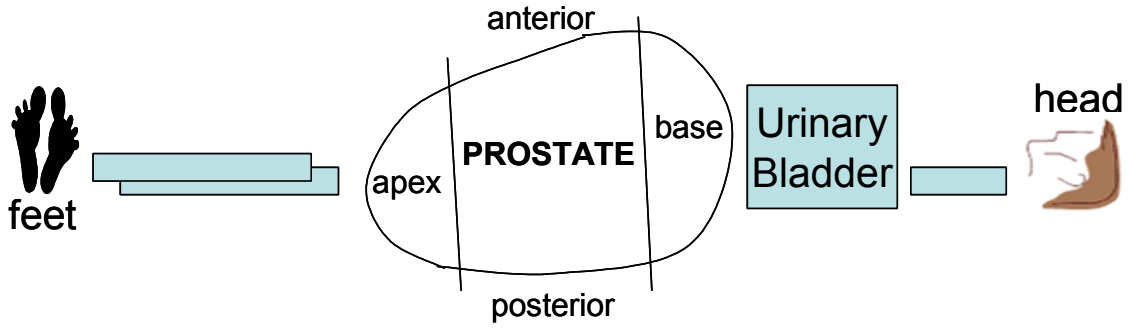

Fig. 2. Prostate Gland and its orientation within the human body

Figure 3 is a transverse view of the prostate gland taken from a slice orthogonal to the urethra. A slice taken in this manner frequently reveals a distinctive apple shape to the prostate. The sometimes distinctive arrow shape of the urethral wall can be seen in the center of the slice. The prostatic glandular epithelial elements are part of the prostate gland and they are the histological compartments where cancer originates (Fig. 3). Later, we will discuss the use of an imaginary line surrounding those glandular elements which we will call the parenchymal contour.

In order to automatically identify the contour of the gland within each prostate slice and replace the arduous and costly manual process, a software algorithm will need to be developed that recognizes the prostate gland capsule utilizing these elements of anatomy and shape.

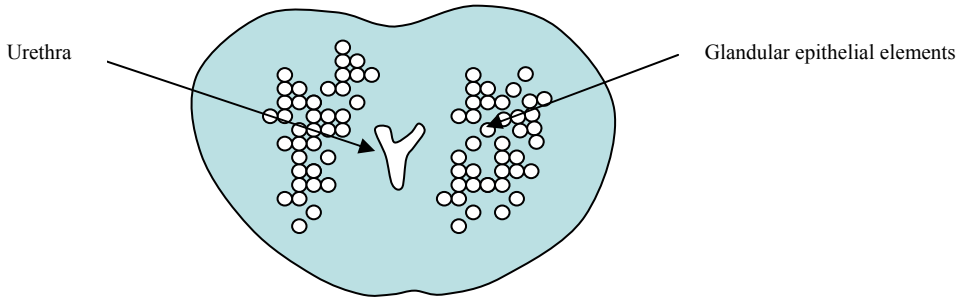

Fig. 3. Prostate anatomy

Certain anatomical features make capsule generally detectable; however, the prostate capsule is unrecognizable in some areas because of the naturally occurring intrusion of muscle into the prostate gland at the anterior apex and fusion of extraprostatic connective tissue with the prostate gland at its base. At these regions where the prostate capsule disappears, its contours will need to be reproduced by drawing a continuing contour line from those areas where the capsule can be objectively recognized and based on the natural shape of the prostate gland.

So far we are unaware of any research that automatically detect the prostate capsule, however some efforts were reported in literature to detect the prostate boundary that separates the prostate from the surrounding body organs. Some researchers used edge-based boundary detection methods that locate edges that correspond to local peaks in the intensity gradient of an image, while others used texture-based methods that characterize regions of an image on the basis of measures of texture. For example, Pathak et al [2] used an edge-based technique for outlining prostate boundary in ultrasonic images. The image's contrast was enhanced first then smoothed by a filter, and then some prior knowledge of the prostate shape and its appearance in ultrasonic images was used to detect the most probable prostate edges. The detected edges were overlaid on top of the image and then presented as a visual guide to the observers for manually delineating the prostate boundary. Liu et al [3] used an edge-based technique as well called radial bas-relief (RBR) method, which is extended from a darkroom technique used in conventional photography, to segment the prostate boundary from ultrasound images. However, the RBR method would fail if the image center and the object boundary centroid have a big deviation. Richard and Keen [4] presented a texture-based method that uses a pixel classifier and a clustering procedure to segment the image to different regions. The reader can refer to Shao et al [5] for a review of the current prostate boundary detection techniques. Although edge detection and texture recognition techniques have been used for the automatic delineation of prostate boundary, determining the prostate capsule cannot be completely solved by only applying such clean cut techniques. This is because the capsule detection depends on many factors like recognizing the histological pattern of the elastic and collagenous fibers within the prostate capsule, urethra location, parenchymal contour location, as well as the whole shape.

In this paper, a mathematical model will be introduced that provides a standard prostate shape. This mathematical model will be used in conjunction with Generalized Hough Transform (GHT) to detect the prostate boundary as well as approximating the missing parts of the capsule where it disappears to a standard shape.

2. GENERALIZED HOUGH TRANSFORM (GHT)

Generalized Hough transform (GHT) was proposed by Ballard [6] to detect shapes of no simple analytical form in which a look-up table is used to define the positions and orientations of boundary points with respect to a reference point. The edge direction at each pixel is measured and the corresponding position vector is retrieved from the lookup table then the cell that represents the reference position in the Hough domain is increased. Figure 4 shows the relevant geometry and the table shows the form of the lookup table where (x_c,y_c) is reference point, (x,y) is an edge point, β is the edge point direction, ϕ is the edge point orientation and r is the distance between the edge point and the reference point.

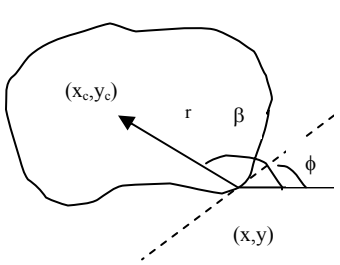

ϕ	(β,r)
ϕ_1	$\{\beta_{11}, r_{11}\}$, $\{\beta_{12},r_{12}\},\{\beta_{13},r_{13}\},\ldots$
ϕ_2	$\{\beta_2, r_2\}$
…	…

Fig. 4. An illustration of GHT parameters and lookup table

Using figure 4, the GHT algorithm can be summarized in the following steps

A- Examine the boundary points of a standard shape to construct the lookup table
   1- Choose a reference point x_c,y_c for the shape
   2- For each boundary point (x,y), find ϕ, β, and find r where $r = (x_c,y_c) – (x,y)$
   3- Store r, β as a function of ϕ
   4- The lookup table is constructed where ϕ is its index and each ϕ may have many values of r, β

B- Applying Hough transform to the image
   5- For each edge pixel (x,y) in the image
      a. Find the entry in the lookup table that corresponds to its ϕ
      b. Increment all corresponding points a = (x,y) + r and store the result in accumulator A
   6- Find maxima in A
   7- Map each maxima back to image space

Hough transform has been used to detect objects of regular shapes in medical images. For example, Solaiman et al [7] has applied Hough transform to locate the aorta in ultrasound images. Fitton et al [8] used Hough transform to automatically assess the regional systolic thickening of the left ventricle from cardiac wall segmentation, where they approximated the shape of the epicardial contour with a circle. Hough transform was used to detect the circle parameters and then number of control points were uniformly placed along the estimated circle boundary for further boundary refinement. Because of the irregular shape of the prostate, Hough transform can not be used in our research; we need a general algorithm that can deal with irregular shapes. Fortunately, generalized Hough transform proved success in detecting objects of irregular shapes [9, 10, 11] and it is applicable to our problem.

3. ESTIMATING PROSTATE CAPSULE USING SHAPE INFORMATION AND GHT ALGORITHM

The main objective of this research is detecting the prostate capsule boundary. However, this boundary is often times unrecognizable because of the naturally occurring intrusion of muscle into the prostate gland at the anterior apex and fusion of extraprostatic connective tissue with the prostate gland at its base. At these regions where the prostate capsule disappears, its contours will be arbitrarily reconstructed by drawing a continuing contour line at those areas where the capsule can be objectively recognized and based on the natural shape of the prostate gland. Section 3.1 will define a mathematical model that provides a standard shape for the prostate, and then section 3.2 will use this model in conjunction with GHT to detect the prostate capsule boundary.

3.1 A Mathematical model for a standard prostate shape top down anterior to posterior

In general, any prostate has a standard shape as the one shown in figure 5 where it has different parameters. This shape can be defined in terms of four curves' equations one in each quadrant as follows

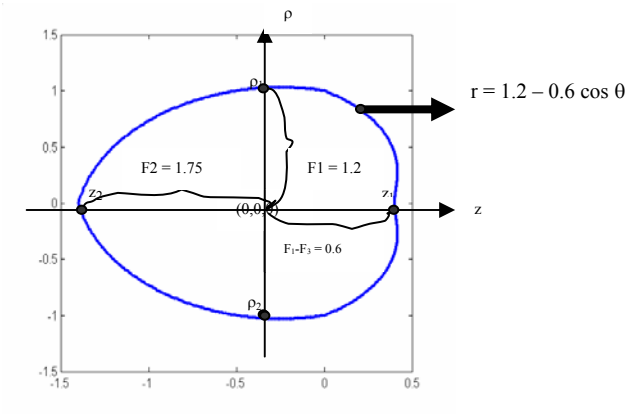

Fig. 5. A standard prostate shape

In the first quadrant, the curve's equation can be defined in terms of two equations

$$z = (F1 - F3\cos\theta)\cos\theta$$
$$\rho = (F1 - F3\cos\theta)\sin\theta$$

Where $0 \le \theta \le \pi/2$

For the second quadrant where $\pi/2 \le \theta \le \pi$

$$z = \left(\frac{2}{\Pi}(F2 - F1)\theta + 2F1 - F2\right)\cos\theta$$
$$\rho = \left(\frac{2}{\Pi}(F2 - F1)\theta + 2F1 - F2\right)\sin\theta$$

Similarly, the third and fourth quadrants curves can be defined by considering the shape's symmetry

The anterior/posterior ratio will be defined as R where R is equal

$$R = \frac{Z1}{-Z2} = \frac{F1 - F3}{F2}$$

Where

$$F1 = \rho_{\max}$$

$$F2 = \frac{\Delta z_{\max}}{1+R}$$

$$F3 = \rho_{\max} - \left(\frac{R}{1+R}\right)\Delta z_{\max}$$

And

$$\rho_{\max} = F1$$
$$\Delta z_{\max} = F1 - F3 + F2 = \rho_{\max} - F3 + F2$$

Up to this point, a standard shape of a complete prostate gland was considered. We now need to find a standard equation that defines a prostate slice. A prostate slice can be viewed as shown in figure 6 where a standard equation can be defined as follows

$$\left(\frac{x}{F}\right)^2 3.32552 + (\frac{y}{F}1.8142857 - 0.27)^2 = 1 \qquad \text{---------- (1)}$$

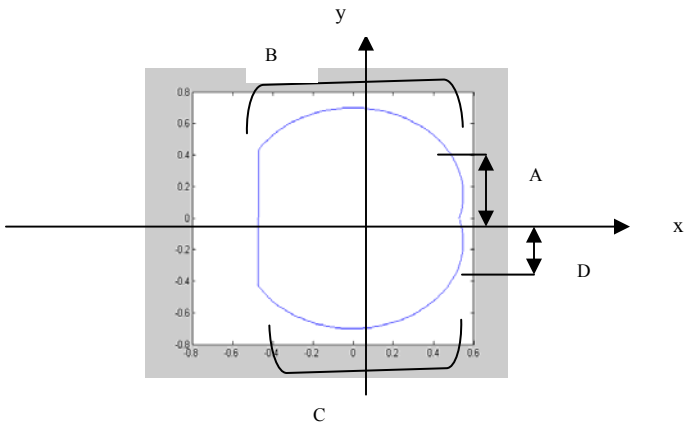

Fig. 6. A standard shape of a prostate slice

Notice that figure 6 consists of four curves marked as A, B, C and D where each of these curves represents a case of equation 1 with different parameters values.

For curve A equation, substitute in equation 1 with y from 0 to 0.1488188F, and find x

Therefore x = $F \times \sqrt{\dfrac{1-\left(\dfrac{1.8142857}{F}y - 0.27\right)^2}{3.32552}}$ ---------- (2)

For curve B, substitute with y = [0.1488188+0.55118 sinθ] F for x;

Where $0<\theta<0.83\pi$

$$x = \pm F \times \sqrt{\frac{1-\left(\frac{1.8142857}{F}y - 0.27\right)^2}{3.32552}}$$ + for $0<\theta<\pi/2$, - for $\pi/2<\theta<0.83\pi$ -------- (3)

For curve C, substitute with y = [0.1488188 - 0.55118 sinθ] F for x;

Where $0.17<\theta<\pi$

$$x = -F \times \sqrt{\frac{1-\left(\frac{1.8142857}{F}y - 0.27\right)^2}{3.32552}}$$ - for $0.17\pi<\theta<\pi/2$, + for $\pi/2<\theta<\pi$ ---------- (4)

For curve D, substitute with y = -0.1488188 F to 0 for x;

$$x = F \times \sqrt{\frac{1-\left(\frac{1.8142857}{F}y + 0.27\right)^2}{3.32552}} \qquad \text{---------- (5)}$$

3.2 GHT and prostate mathematical model

GHT can be applied to detect the prostate boundary by the use of prostate slice equations defined in the previous section as follows

For a prostate slice

1. Choose a reference point x_c,y_c for the shape (It can be the central point)
2. For each boundary point $y = (x_i,y_i)$, find r where $r = (x_c,y_c) – (x_i,y_i)$ then substitute with y in equations 2,3,4, or 5 (according to the current quadrant) to get the corresponding curve equation x
3. Store r, y, and x in a lookup table (Table 1)
4. For each r in the lookup table, count the number of points that construct each curve occurrence and represent the counter by c
5. Choose the largest c for each r; this represents the strongest curve occurrence.

r	(x,y)
r_1	$\{x_{11},y_{11}\}$, $\{x_{12},y_{12}\}$,$\{x_{13},y_{13}\}$,…
r_2	$\{x_2, y_2\}$
…	…

Table 1. A lookup table for the proposed GHT

Determining the boundary points in step 2 of the previous algorithm can be done by recognizing the histological pattern of the elastic and collagenous fibers within the prostate capsule (Wavy lines being pointed to by arrows in figure 7a). This can be clearly recognized under the microscope but also under high resolution of the scanned digital images. The locations of these wavy lines will be the input to the GHT algorithm. In order to correctly locate those lines, it is essential to detect the parenchymal outer contour of the prostatic glandular epithelial elements illustrated in fig. 3, since the capsule has to be above this line. The thin yellow line in Figure 7b illustrates this parameter in an actual prostate slice. The detection of the wavy lines and the parenchymal line can be done using a texture based segmentation method [4, 12] which we will be report in details in future publications.

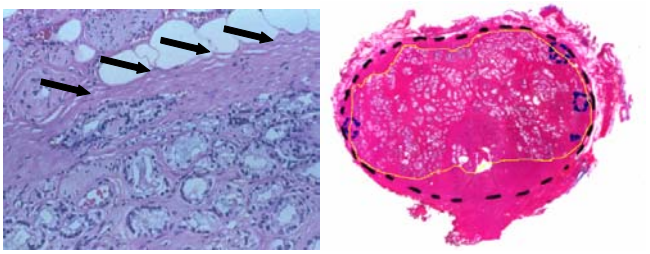

(a) (b)

Figure 7: (a) Histological pattern of elastic fibers within prostate capsule, (b) Parenchymal Outer Contour

4. RESULTS

Results to date are presented below in Table 2. Those results were obtained by using the “whole mount” slicing technique and by using the hand-drawn contours. The reader can refer to McKenzie et al [1] for a complete description

of the percentage of coverage calculation method. The final two rows in the table provide the percentage of coverage using point clouds at different densities with the denser point cloud providing a bound of the coverage at between 80.1 and 84.7% extracapsular tissue coverage. We believe that our proposed algorithm will illuminate errors that have been contributed by human judgments and incorrect handling as well as it will significantly speed the processing time of specimens. The new results will be reported in future publications.

	Model constructed using 50*50*100 divisions	Denser point cloud using 100*100*200 divisions
# Of original gland points	1864	15201
# Of original fat points	2437	19750
# Of gland points on the surface	356	1542
# Of covered points (4 basic neighbors)	263	1235
# Of covered points (8 basic neighbors)	286	1306
% Coverage (by checking the 4 basic neighbors of the point)	73.8764	80.0908
% Coverage (by checking the 8 basic neighbors of the point)	80.3371	84.6952

Table 2. Percentage of coverage of extraprostatic tissue using two point clouds at different densities

5. CONCLUSION

An accurate assessment of the percentage and depth of extra-capsular soft tissue removed with the prostate by the various surgical techniques can help surgeons determining the appropriateness of surgical approaches. In order to facilitate the reconstruction phase and thus provide a more accurate quantitation results when analyzing the images, it is essential to automatically identify the capsule line that separates the prostate capsule tissue from its extra-capsular one. 3D edge detection and pattern recognition techniques have been used for the automatic delineation of neighboring tissues in medical data. However, since determining the prostate capsule depends on many factors like the wavy patterns, urethra location, parenchymal line as well as the shape, it cannot be completely solved by only applying such clean cut techniques. In this paper, we presented a novel algorithm to detect the prostate capsule boundary with the use of generalized Hough Transform (GHT) and prostate shape equations. Quantitation results are expected to be improved by applying this algorithm.

Our future efforts will be directed towards investigating various image processing techniques to detect the histological wavy pattern of the elastic and collagenous fibers within the prostate capsule as well as the identification of the loose connective tissue and fat present in the extraprostatic tissue immediately out of the capsule. This investigation will be reported in future publications.

REFERENCES

1. McKenzie, Frederic D., Rania Hussein, Jennifer Seevinck, Paul Schellhammer, Jose Diaz. “Prostate Gland and Extra-Capsular Tissue 3D Reconstruction and Measurement.” The 3rd IEEE symposium on Bioinformatics and Bioengineering (BIBE), Bethesda, Maryland. March 10-12, 2003. Pages 246-250.
2. Pathak SD, Haynor DR, Kim Y. “Edge-guided boundary delineation in prostate ultrasound images.” *IEEE Transactions on Medical Imaging*; **19(12)**, pp.1211-19, 2000.

3. Liu YJ, Ng WS, Teo MY, Lim HC. “Computerised prostate boundary estimation of ultrasound images using radial bas-relief method.” *Medical & Biological Engineering & Computing*; **35(5)**, pp.445-54, 1997.

4. Richard WD, Keen CG. “Automated texture-based segmentation of ultrasound images of the prostate.” *Computerized Medical Imaging & Graphics*; **20(3)**, pp.131-40, 1996.

5. Shao F, Ling KV, Ng WS, Wu RY. “Prostate boundary detection from ultrasonographic images: review article”, *J Ultrasound Med*.; **22(6)**: 605-23, 2003

6. D.H. Ballard, “Generalizing the Hough transform to detect arbitrary shapes”, *pattern recognition* **13(2)**, 111-122, 1981

7. Solaiman B, Burdsall B, Roux C. “Hough transform and uncertainty handling. Application to circular object detection in ultrasound medical images.” Proceedings 1998 International Conference on Image Processing. ICIP98 (Cat. No.98CB36269). IEEE Comput. Soc. Part vol.3, 1998, pp.828-31 vol.3. Los Alamitos, CA, USA.

8. Fitton I, Shen J, Perron J-M, Kerouani A, Roudaut R, Barat J-L. “Regional myocardial wall thickening of the left ventricle from segmentation of echocardiographic images.” SPIE-Int. Soc. Opt. Eng. Proceedings of Spie - the International Society for Optical Engineering, **vol.4549**, 2001, pp.58-63.

9. Wong KC, Sim HC, Kittler J. “Recognition of two dimensional objects based on a novel generalized Hough transform method.” Proceedings. International Conference on Image Processing (Cat. No.95CB35819). IEEE Comput. Soc. Press. Part vol.3, 1995, pp.376-9 vol.3. Los Alamitos, CA, USA.

10. Du-Ming Tsai. “An improved generalized Hough transform for the recognition of overlapping objects.” *Image & Vision Computing*, **15(12)**, Dec. 1997, pp.877-88.

11. Pui-Kin Ser, Wan-Chi Siu. “A new generalized Hough transform for the detection of irregular objects.” *Journal of Visual Communication & Image Representation*, **6(3)**, Sept. 1995, pp.256-64.

12. Karssemeijer N. “Automated classification of parenchymal patterns in mammograms.” *Physics in Medicine & Biology*, **43(2)**, Feb. 1998, pp.365-78.